Wigner function simulation of intrinsic oscillations, hysteresis, and bistability in resonant tunneling structures

Bryan A. Biegel

NASA Ames Research Center, Moffett Field, CA 94035-1000

ABSTRACT

Several interesting behaviors of resonant tunneling diodes (RTDs) are investigated through numerical simulation: high frequency self-oscillations, strong intrinsic hysteresis, and pronounced static bistability. Each of these behaviors has been observed experimentally in RTDs, but the measured effects have been slower (oscillations), weaker (hysteresis, bistability), or required external inductance to occur (oscillations, hysteresis). These simulations indicate that the effects occur strongly and intrinsically in an RTD when a narrow energy band in the emitter aligns just below a quantized energy state in the quantum well. Quantum system models and available computation power have only recently developed to a point where the necessary physical effects (inelastic scattering, self-consistency, and transient operation) can be properly included to simulate these behaviors in a quantum device. A 1-D Wigner function model is used for transient, self-consistent RTD simulations including inelastic scattering. 1-D transfer-matrix calculations are used to locate quantized energy levels. The physics behind the intrinsic oscillations, hysteresis, and bistability are described for the simulated RTD. Simulation results are also presented for double-well RTD structures in an attempt to enhance these effects.

Keywords: Wigner function simulation, resonant tunneling diodes, self-oscillation, bistability, hysteresis

1. INTRODUCTION

Resonant tunneling diodes (RTDs) [1-3] have undergone intense experimental and theoretical investigation over the past decade and more, due to their potential circuit applications [2, 4] and their status as a prototype quantum electronic device. Several potentially useful behaviors have been observed in RTD measurements, including high-frequency oscillations [5 -8], hysteresis in the current-voltage (I-V) curve [5, 7, 9], and intrinsic bistability [10-12]. In 1991, Jensen and Buot (JB) [13] described some ambitious RTD simulations which showed all of these effects in a single device for the first time. In [13] and subsequent theoretical analysis of these simulations by Buot et al. [14-19], the physics and circuit implications of this simulated behavior was analyzed in great detail. Significantly, that analysis contradicted some of the consensus views of the physics of these phenomena in RTDs.

This work revisits the simulation of the JB RTD in greater detail, to re-evaluate the physics of this device and to explain any discrepancy between simulation and experimental results. The steady-state operation of the device is analyzed in Section 2, and the transient operation in Section 3. Section 4 analyzes the sensitivity of these effects to various practical considerations, and presents simulations of double-well RTDs which attempt to enhance the plateau effects for more robust operation. Both Wigner function [20, 21] and transfer-matrix [22, 23] simulation capabilities of SQUADS (Stanford QUAntum Device Simulator) [24, 25] were used in this work.

2. STEADY-STATE RTD PHYSICS

The RTD simulated by Jensen and Buot has a very basic structure, as shown in Figure 1. It is composed of a 5 nm undoped GaAs quantum well between 3 nm undoped $Al_{0.3}Ga_{0.7}As$ tunnel barriers and 3 nm undoped GaAs spacer layers. The GaAs contact layers (doped n-type at $2 \times 10^{18}/cm^3$) are 19 nm each, giving a total device width of 55 nm. To facilitate comparison to the simulations of JB [13], identical simulation parameters are used: electron effective mass of $0.0667 m_0$, permittivity of $12.9 \varepsilon_0$, effective relaxation time of 525 fs [26], and a simulation temperature of 77 K. Also as in [13], all Wigner function simulations include self-consistency and scattering, use position grid spacing of 0.647 Å and 72 wavenumber points, and use a time step of 1 fs (for transient simulations).

The fundamental operation characteristic for electronic devices is the current-voltage curve, so this will serve as the starting point in this investigation of the JB RTD. A Wigner function simulation tracing the steady-state I-V curve of this RTD is
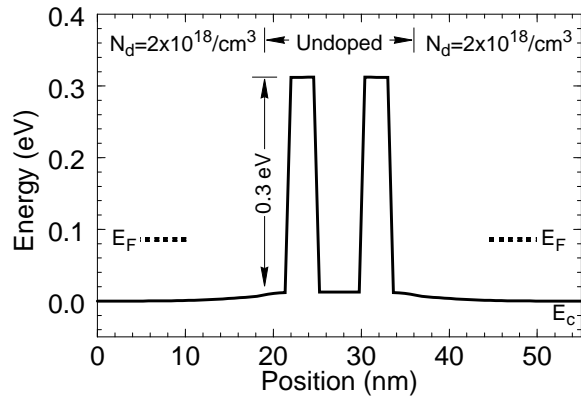
Figure 1: Simulated Jensen and Buot (JB) RTD structure [13]: equilibrium self-consistent conduction band $E_c(x)$, Fermi levels E_F, and doping $N_d(x)$. The 0.3 eV $Al_{0.3}Ga_{0.7}As$ tunnel barriers are 3 nm thick, and the GaAs quantum well width is 5 nm. The center 17 nm of the device is undoped.
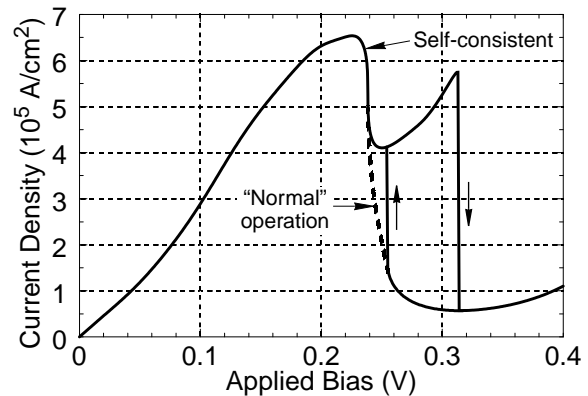
Figure 2: Self-consistent, steady-state (equilibrium operating point) RTD I-V curve, showing an upward-sloping plateau and hysteresis in the NDR region. "Normal" RTD operation (without the plateau) is indicated by the dashed curve.

shown in Figure 2. To explain the physics behind the more interesting features of this I-V curve, a brief review of basic RTD physics is useful. The key feature of the basic RTD I-V curve is a region of negative differential resistance (NDR). The cause of NDR is indicated in Figure 3, which shows the conduction band profile of the JB RTD at both the peak and valley of the I-V curve. At applied biases up to and including the peak current condition (0.23 V in the JB RTD), electrons entering the RTD at the emitter contact can tunnel through the double-barrier structure via the quantum well state (QWS). As the bias is increased above the peak condition, the QWS energy drops below the emitter band edge, and current decreases due to a greatly reduced tunneling probability. This "normal" RTD behavior is well described in [2] and elsewhere.

Figure 2 shows that the simulated JB RTD does not behave in the simple manner described above in the NDR region of operation. Instead of the current falling smoothly from peak to valley, a plateau structure occurs in the NDR region of the I-V curve. The plot in Figure 4 of the conduction band profile of the RTD at 0.28 V (the center of the plateau) indicates that a new current path is active. At this bias, the QWS is indeed well below the band minimum at the emitter contact, so electrons entering the RTD at the emitter can not tunnel through the QWS directly. However, an extended potential depression has developed in the emitter conduction band. It appears that the plateau current results from electrons scattering into the emitter depression and then tunneling through the QWS to the collector. Since the emitter depression is narrow (10-20 nm), the quantum mechanically allowed energy levels (below E=0) for electrons will be discrete and widely separated, just as in the quantum well. Thus,
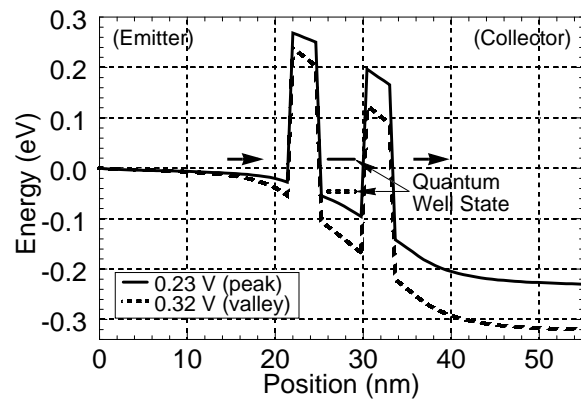
Figure 3: Peak and valley conduction band profiles. Carriers entering from the emitter can tunnel through the quantum well state at the bias for peak current (0.23 V), but not at the bias for valley current (0.32 V).
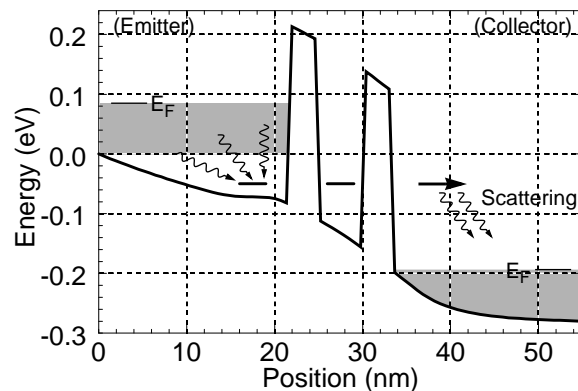
Figure 4: Self-consistent RTD conduction bands at the center of the I-V plateau (0.28 V). Electrons must scatter into the discrete energy state in the emitter depression to tunnel through the quantum well state.

this explanation for the plateau effect depends on a quantized state in the emitter depression being at roughly the same energy as the QWS, so that current can flow from the emitter state to the QWS.

To verify that the plateau is due to an alignment of quantized energy states, the transfer-matrix method (TMM) capability of SQUADS is used to locate resonant energy levels in the device. Rather than searching for energy states at $E > 0$ where a peak in the transmission coefficient occurs, the TMM is modified to find resonant energies at $E < 0$, corresponding to wavefunctions with the highest standing-wave amplitudes in the emitter depression and quantum well. Using this approach, Figure 5 shows the resulting energy spectrum (normalized wavefunction amplitude versus energy) of carriers in the emitter depression (solid curve) and quantum well (dashed curve) for RTD operation at the center of the plateau (0.28 V). The first discrete emitter state (DES) energy is only about 5 meV below the QWS energy, which is close enough for these states to interact and transmit a significant current.

Note that the DES and QWS energies are separated by only 5 meV at the center of the plateau, yet the plateau extends over about 75 mV of applied bias. This requires that the two energy levels stay essentially "locked" together during the plateau portion of the I-V curve: any changes in energy must be virtually equal. This is exactly what occurs: the DES/QWS separation starts at just 8 eV at Va = 0.24 V, and the DES energy increases slowly with applied bias until it rises above the QWS energy at the end of the plateau. In fact, plateau operation is only maintained if the DES is energetically below the QWS. With the QWS above the DES, if the QWS charge density increases, the electrostatic field in the collector barrier increases while that in the emitter barrier decreases, so the potential of the QWS rises further above the DES. This reduces the current flow from DES to QWS, reducing the QWS charge. By symmetry, as the QWS charge decreases, the potential of the QWS decreases towards the DES energy, so the supply of electrons from DES to QWS increases, and the cycle repeats. Thus, a restoring mechanism due to charge storage in the quantum well keeps the QWS slightly above the DES. However, if the DES ever rises above the QWS, the supply of electrons to the QWS decreases, and the QWS begins to deplete. The potential of the QWS drops further below the DES. This further reduces the supply of electrons to the QWS. A run-away conditions ensues, which ends when the lower I-V curve operating conditions are reached.

The fact that the QWS energy does not rise with respect to the collector band minimum indicates that the conduction band profile in the collector and quantum well does not change appreciably through the plateau. Therefore, all increases in applied bias must be accommodated by band-bending in the emitter. Figure 6, which shows the RTD conduction band profile for consecutive biases in the plateau, verifies this. This also indicates that the total charge in the quantum well and collector remains constant throughout the plateau. If the charges changed appreciably, then the electric fields in the device would also be modified, as would the potential profile. Again, plots of total charge in the collector and QW versus applied bias [27] confirm this.
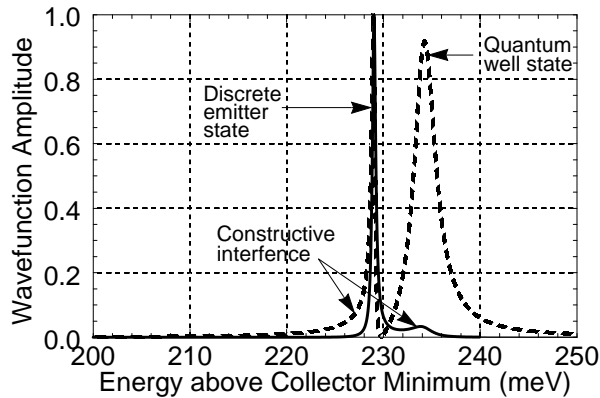
Figure 5: Energy occupation spectrum (normalized wavefunction amplitude versus energy) of carriers in the emitter depression (solid curve) and quantum well (dashed curve) for the conduction band diagram of Figure 4. The first emitter energy level is only about 5 meV below the quantum well state. Constructive interference is apparent near the respective resonant energies, and destructive interference between.
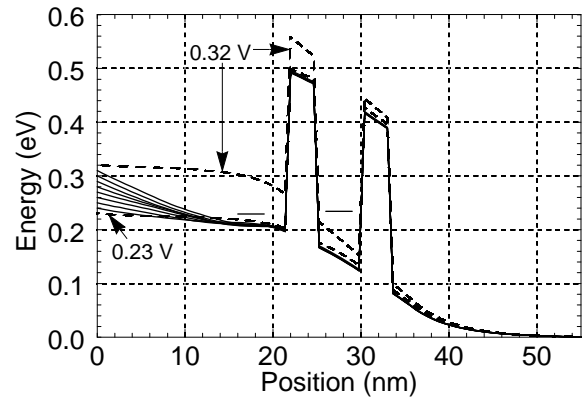
Figure 6: Self-consistent conduction band profile for the plateau (solid curves) and adjacent biases (dashed curves). All applied bias changes in the plateau are accomodated by charging of the emitter contact and discharging of the emitter itself. The resonant states at the center of the plateau (0.28 V) are shown in the emitter depression and quantum well.

These results also indicate that current through the DES/QWS path remains constant through the plateau. Therefore, the positive slope of the plateau must be attributed to current from unscattered electrons, which see rapidly lowering tunnel barriers as bias increases in the plateau (see Figure 6). Previous explanations [14] of the positive slope in the I-V plateau of this RTD were much more complicated.

In summary, the physics of the I-V plateau and associated hysteresis can be described as a collaboration of several phenomena: scattering, the development of a potential depression in the emitter, the alignment of a discrete emitter state with the quantum well state, and charge storage in the quantum well. On the up-trace, as the QWS drops below 0 (*i.e.*, the emitter contact conduction band minimum) after the peak condition, the quantum well begins to deplete. Normally, the emitter charge increases to compensate, but a lower-energy means accommodating the applied bias exists in this case: the development of a potential depression in the emitter. A discrete emitter state develops in this emitter depression which electrons scatter into, and which provides a current path through the slightly higher energy QWS. A negative feedback mechanism due to quantum well charge keeps the QWS slightly above the DES as the bias increases. Thus, current through the DES-QWS current path remains essentially constant throughout the plateau. However, current due to electrons which do not scatter into the DES increases with bias as their energy rises toward the top of the barriers. Also with increasing bias, the DES is slowly pushed up towards the QWS. When the two states cross, the electron supply from DES to QWS decreases, the QWS energy drops as it depletes, and the plateau ends abruptly. On the down-trace, the QWS is initially empty, and the bias must be decreased to where the QWS is just below the emitter energy before electrons from the emitter began to scatter into the QWS, raising its potential, and returning the RTD to plateau operation. Thus, quantum well charge is solely responsible for the plateau's hysteresis, as determined by JB [13].

3. TRANSIENT RTD PHYSICS

We now turn from steady-state to transient physics of the I-V plateau in the JB RTD I-V curve. This begins with a transient Wigner function simulation trace of the I-V curve, similar to simulations of Jensen and Buot [13]. [Figure 2 is a steady-state curve, which traces the (stable or unstable) equilibrium operating point.] Like Jensen and Buot, these transient simulations showed high-frequency current oscillations at fixed biases throughout the plateau after switching from one applied bias to the next. However, for biases above about 0.25 V, the plateau is actually stable, since the oscillations decayed and the device eventually reached steady-state. Very long transient simulations showed that the JB RTD is unstable in the plateau only at biases of 0.25 V and below, in contrast to the conclusion of JB [13] that the entire plateau was unstable. For example, Figure 7 shows the current oscillations at 0.24 V after they have converged to a steady waveform and amplitude after about 20 ps. These are quite large (and therefore potentially useful) oscillations, with a frequency of about 2.5 THz and an amplitude of 1.8×10^5 A/cm^2, which is over 40% of the time-average current.

The transient I-V curve was identical to the steady-state curve where the RTD was stable. However, in the small range of
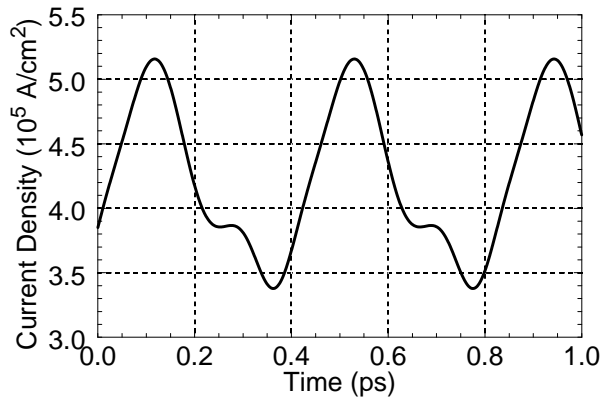
Figure 7: 2.5 THz intrinsic current oscillations at an applied bias of 0.24 V in the JB RTD. The oscillations result from the changing relative positions of the energy states in the emitter depression and the quantum well.
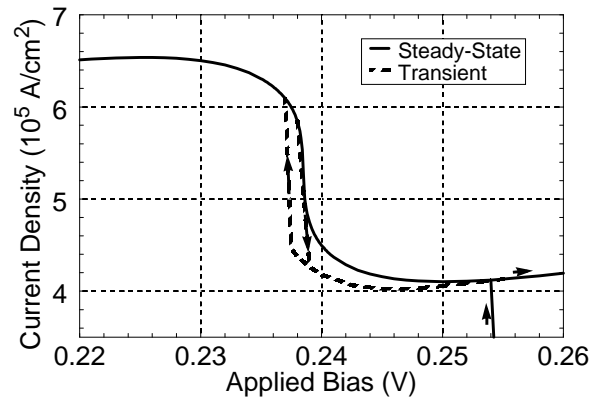
Figure 8: Steady-state (equilibrium) and transient (time-averaged) I-V curve detail near the upper transition to the plateau. The transient I-V curve has a second, dynamic hysteresis loop near the main peak of the I-V curve.

biases where there were perpetual oscillations (i.e., where the transient simulations did not converge to steady-state), the time-average current was not equal to the (unstable) equilibrium value found by the steady-state simulation. In that region of operation, since the transient simulation follows the actual evolution of the device, and since experiments typically measure time-average current, the transient I-V curve is the physically correct one. Figure 8 shows a detail view of unstable region of the equilibrium steady-state and the time-average transient I-V curves. In following the down-trace of the transient I-V curve, a second hysteresis loop not seen in the steady-state simulation was discovered. Thus, three features of the transient operation of the JB RTD need to be investigated: the cause of the oscillations, the physical difference between the lower (unstable) and upper (stable) portions of the plateau, and the cause of the second hysteresis.

Considering the unstable oscillations, the discussion of restoring mechanism in the previous section suggests that time-dependent variations in the alignment of the DES and QWS due to charge density variations might produce this effect. To confirm this, Figure 9 shows charge density and conduction band profiles for the minimum and maximum current conditions of Figure 7. To see charge variation more clearly, Figure 10 shows integrated charge in the emitter and quantum well versus time. Thus, during oscillations, the emitter and quantum well charges oscillate about 180 degrees out of phase with each other, resulting in a similar oscillation in the alignment of the DES and QWS. This confirms the restoring mechanism (more precisely, a "limit-cycle" mechanism [14] in this case) described in Section 2 as the cause of plateau oscillations. This description of the oscillation physics of the JB RTD largely agrees with that of Buot and Rajagopal [16, 17], although "DES energy" must replace "Fermi level" in their description.

The possibility of oscillations occurring in an RTD where a discrete emitter state charges the QWS was first predicted by Ricco and Azbel [28]. However, they did not foresee that the DES must remain below the QWS for the restoring mechanism (self-consistency) to maintain this current path. They also suggested that an RTD would never reach steady-state under these circumstances. However, the transient I-V trace showed that this RTD *is* stable in the upper portion of the plateau. This brings us to the second interesting feature of the transient I-V trace: that the plateau is partly stable and partly unstable. The reason is that unstable operation requires a negative differential resistance (NDR) effect. Thus, for plateau operation at biases of 0.25 V and below, the RTD will be unstable, while above 0.25 V it will be stable. [Note that the JB RTD is not unstable in the NDR portion of the lower I-V curve because the oscillatory mechanism discussed above is not operational except in the plateau. In particular, for operation along the lower I-V curve in Figure 2, there is essentially no charge in the QWS, and no DES.]

Finally, the third interesting feature of the transient I-V curve of Figure 8 is the narrow hysteresis loop just below 0.24 V. Since there is no hysteresis in the steady-state I-V curve in the main current peak, the cause of this hysteresis must be a dynamic effect. Indeed, the RTD is oscillating here on the transient down-trace. Plots of the current oscillations [27] show that the RTD is not oscillating around the equilibrium operating point in the steady-state I-V trace. The oscillations somehow allow the RTD to remain in plateau operation (i.e., with an emitter depression and DES/QWS current path) longer than a non-oscil-
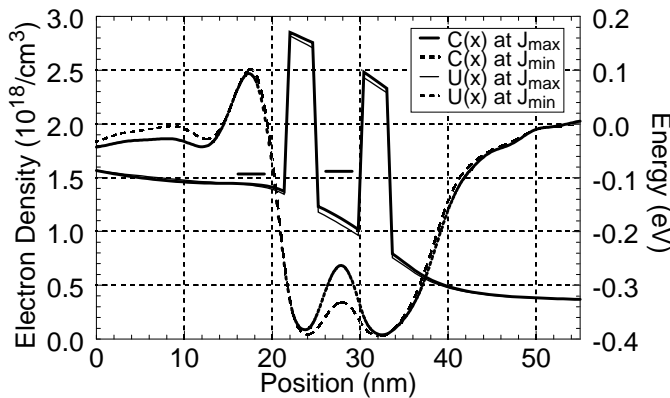
Figure 9: Self-consistent conduction band and electron density during oscillations at 0.24 V. The solid curves correspond to the maximum current; the dashed curves to the minimum. The quantum well potential (and thus the quantum well state energy) only varies by about 12 meV.
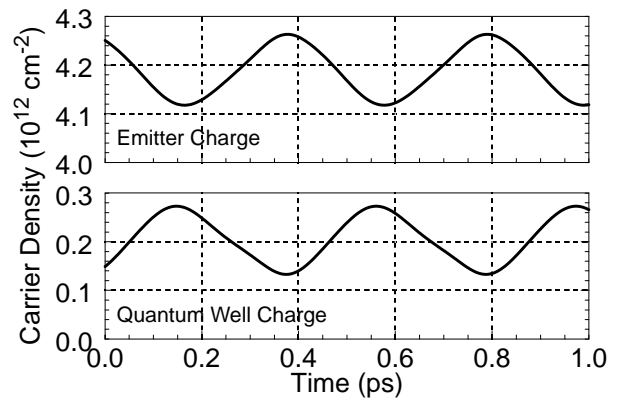
Figure 10: Total (integrated) charge in the emitter layer (top) and quantum well (bottom) versus time during oscillations at 0.24 V bias. Self-consistency tries to maintain a constant net charge in the device, so a decrease in one region causes an increase in the other, and vice-versa.

lating RTD does. This I-V curve feature has been shown in RTD equivalent circuit simulations and experimental measurements previously [5, 7, 29, 30]. Sollner [5] used a kind of momentum argument to explain this form of hysteresis: "it is necessary to bias the diode nearer the region of maximum negative conductance to begin oscillations...than to suppress oscillations after they have begun...." Wallis and Teitsworth [31, 30] use the term "subcritical Hopf bifurcation" for this effect. This appears to be the first definitive demonstration of dynamic hysteresis in intrinsic RTD simulations. However, this effect needs to be enhanced (wider hysteresis loop) to exploit it in real devices.

4. DISCUSSION

The plateau effects described above could be used in several applications: a THz oscillator, a microwave detector, a three-state device [25], or other quantum functional devices [4]. In order to develop real devices based on simulations, accuracy of the simulations is critical. Wigner function simulation results such as those described above and elsewhere (e.g., [13, 25, 27]) indicate that this method of quantum device simulation can provide a great deal of insight into the physics of "macroscopic" quantum devices such as the RTD. Indeed, the Wigner function model allows one to include scattering, self-consistency, open boundaries, and transient effects in a computationally feasible simulation. However, some aspects of the JB RTD simulations above raise questions about their accuracy and practical significance. For example, did the emitter depression form simply because the emitter region was so short? What is the effect of enforcing current continuity at the contacts? How sensitive are the plateau effects to changes in the relaxation time or scattering model? And finally, what modifications can be made to the JB RTD to produce the useful plateau effects more robustly? This section will address these questions with further simulations and discussion. [Note that the physical and numerical parameters used in Sections 2 and 3 were identical to those used in [13], so that the physics behind the results in [13] could be illuminated.]

The most obvious possible inaccuracy of the Wigner function simulations in Sections 2 and 3 is indicated by the high electrostatic field at the emitter contact during plateau operation. A high electric field at a contact indicates that the simulation results are not independent of the simulation region boundary location. From a search of the literature, contact layer widths in experimental RTDs are typically 100 to 1000 nm, rather than the 19 nm (chosen to limit computational size [32]) of the JB RTD. Thus, the simulation results of Sections 2 and 3 may say little about the operation of most experimental RTDs. In particular, since the emitter contact electric field was significant for plateau operation, the interesting physics (which all occurred in the plateau) could be entirely a result of the short emitter. To check this possibility, steady-state and transient I-V trace simulations were run with wider emitter layers. The result was that although the plateau effects were diminished, they were all still present in the wide-emitter device. For example, Figure 11 shows the I-V curve for an RTD with a 63 nm emitter, and Figure 12 shows the conduction band profile of the same RTD for operation in the plateau. Increasing the emitter width beyond 40 nm, or the collector width beyond its original 19 nm, had a negligible effect on the I-V curve. These results show that the potentially useful plateau effects are maximized with a narrow emitter (distance between tunnel barrier and metal contact) compared to those in typical experimental RTDs.

Another cause for concern about the accuracy of the foregoing RTD simulations is the use of equilibrium Fermi-Dirac boundary conditions [20], which is standard practice in Wigner function simulations. These boundary conditions assume an equilibrium incoming distribution of carriers from the contact, even though a very high current may exist just inside the simulation region. It would be more physically correct to use boundary conditions which exhibit current continuity with the device. To accomplish this, another steady-state I-V curve was computed for the JB RTD using drifted (i.e., non-zero average velocity) Fermi-Dirac boundary conditions [33]. To achieve current continuity at the boundaries, a second iteration was undertaken outside the Poisson self-consistency iteration. The external iteration ended when the average drift wavevector (velocity) of the boundary conditions changed by less than 0.01% of a wavevector grid space. The resulting I-V trace (not shown here) was very similar to that for equilibrium BCs, and in particular, plateau effects are essentially unchanged. Because of the relatively small effect and the high additional computation required to enforce current continuity at the boundaries, this constraint was not enforced in any other simulations in this work.

Still another issue of concern is the sensitivity of the plateau effects to changes in the relaxation time or scattering model. All published Wigner function simulations to date which included scattering have used the relaxation time approximation scattering model [5, 21]. In the above simulations, the relaxation time was the same as that used by JB [34], to allow direct comparison to their results. The sensitivity of the plateau effects to scattering changes can be investigated by changing the relaxation time directly, changing the temperature of the simulation (which alters both the relaxation time and boundary conditions), or using a different (and presumably more accurate) scattering model than relaxation time. The investigation of more
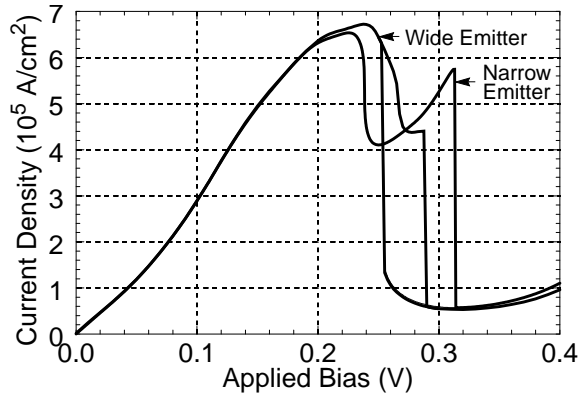
Figure 11: Wide (63 nm) emitter equilibrium I-V curve. The narrow (19 nm) emitter I-V curve is shown for comparison. Using a narrow emitter causes the RTD to begin plateau operation at lower biases and more abruptly, and prolongs it to higher biases, than the wide emitter RTD. However, the I-V plateau still occurs in the wide emitter RTD, and is caused in the same manner as in the narrow emitter RTD.
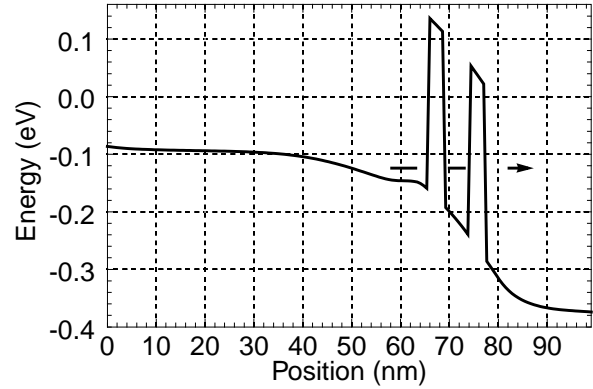
Figure 12: Wide emitter conduction band profile during plateau operation at 0.28 V. Also indicated are the positions of the DES and QWS (from transfer-matrix analysis). Note that the emitter contact e-field is small, as intended. This shows that the formation of an emitter depression and the resulting I-V plateau are not simply the result of inaccurate boundary conditions in the narrow emitter RTD simulations.

accurate scattering models deserves much more space than is available here, so this will be pursued in a future work. This work presents results for both of the other options, as shown in Figures 13 and 14. From these results, we see that the plateau effects are quite dependent on the scattering rate of carriers. At temperatures above 200K, the plateau effects are essentially quenched. At lower temperatures, the plateau effects are stronger, but the region of NDR becomes narrower, so that oscillations will occur over a narrower range of bias conditions. The results are similar for the relaxation time variation. Note that a larger relaxation time means less scattering, which is similar to a lower temperature. Here again we see that if the relaxation time decreases by a factor of two, the plateau is essentially lost. Conversely, if the relaxation time increases by a factor of two, the NDR region of the plateau disappears, so that high frequency oscillations will not occur. The conclusion is that in order to use simulation to design a device to produce these effects, the temperature and scattering model used in simulations must closely match that of the real device.
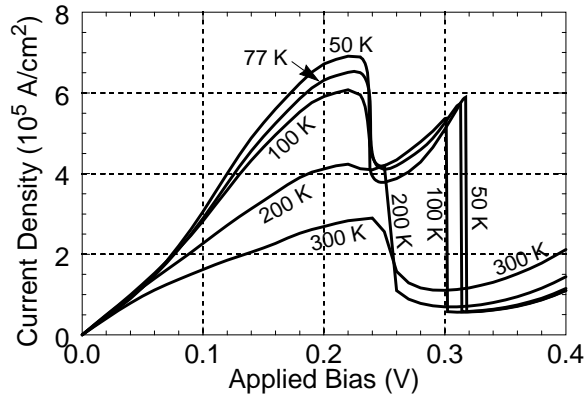
Figure 13: I-V curves for JB RTD versus simulation temperature. Temperature modifies both the relaxation time and the boundary conditions. Note that above 200 K, the plateau effects are quenched, because the emitter conduction band depression does not form. Below 100 K, the plateau effects strengthen only moderately with decreasing temperature.
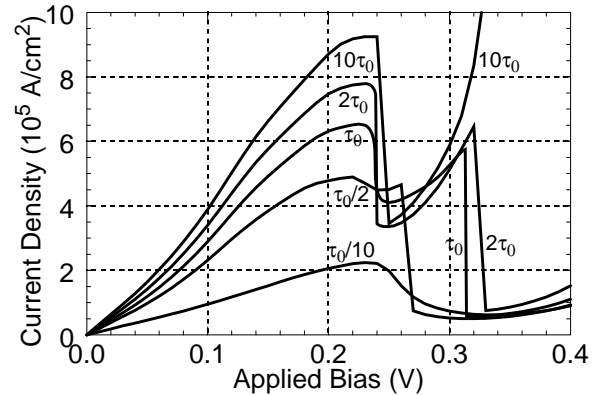
Figure 14: I-V curves for JB RTD versus relaxation time $\tau = a\tau_0$. A larger relaxation time means less scattering. Note that all plateau effects are essentially gone for $\tau < \tau_0/2$. Also, although plateau effects strengthen with increasing τ, the NDR region of the plateau is effectively gone for $\tau > 2\tau_0$. Thus, high frequency oscillations will not occur in that limit.

Several experimental RTD measurements showing effects due to emitter potential wells and resulting discrete emitter states have been claimed or demonstrated [35-38]. These RTDs are usually specially designed to produce these effects, unlike the fairly conventional (except for the narrow emitter) JB RTD. The previous results of this section, especially those concerning variations in the scattering model, indicate that the JB RTD may not produce the plateau effects very reliably. Therefore, a final investigation in this work is to attempt to identify an RTD structure that produces the plateau effects more strongly and robustly. Based on the analysis in Section 2 of the plateau physics, such a device must supply electrons to the main quantum well in two distinct energy bands. The lower of these bands must have a sharp energy distribution centered just below the QWS energy. In the JB RTD, the short emitter and self-consistency cause an emitter depression and DES to form after the current peak, and this DES happens to be just below the QWS energy. There are several ways to *design* an RTD to produce a sharp energy distribution in the emitter, including using a narrow-band material to form a quantum well next to the emitter barrier, inserting a third tunnel barrier (second quantum well) in the emitter, adding a superlattice in the emitter, and inserting a complete RTD structure in emitter. The latter two approaches were not expected to produce an electron beam at an energy below the QWS energy. Results and discussion for the first two approaches follow.

The first approach used to create a quantum well and DES was to insert an InGaAs layer next to the emitter barrier of the JB RTD. Figure 15 shows the conduction band profile of one such structure, in this case with an 8 nm, 5% indium layer. Figure 16 shows the I-V curve for this RTD. The plateau, hysteresis, and bistability are quite evident in the I-V curve. In fact, a second hysteresis loop has opened under the main current peak. Figure 15 shows the conduction band and carrier density profiles for operation in the plateau region (0.3 V bias), indicating that a potential depression still forms in the emitter of this modified device. Note that the DES must align just below the QWS after the current peak, and sufficient electrons must be able to scatter into the DES to keep the QWS full - two very difficult constraints to satisfy. Based on numerous simulations of modified RTDs with InGaAs quantum wells of various shapes and sizes, the collaborative mechanisms in JB RTD seem to be more reliable way to produce the plateau and its associated effects.

The second attempt to enhance the plateau effects of the JB RTD was to insert a tunnel barrier in the emitter, creating a second quantum well just upstream of the first, as shown in Figure 17. The intent was to produce the necessary DES in the new emitter quantum well. Note that producing an I-V plateau requires the QWS to switch from incoming electrons at one energy level to those at another at some point in the I-V curve. In the JB RTD, unscattered electrons create the first I-V peak, and electrons from the DES create the second. In the triple-barrier RTD of Figure 17, the emitter quantum well must be designed very carefully to achieve two energy states at the necessary energies. Design parameters used in these simulations included quantum well width, doping, and indium content, and the use of a graded InGaAs "ramp" to allow electrons to reach low energy levels in the emitter quantum well. Even with all of these design options, an I-V plateau was never produced in simulations of this structure. However, hysteresis and bistability were often quite strong, as shown by the I-V curve in Figure 18 for the triple-barrier RTD of Figure 17. Once again, the simple JB RTD seems the most reliable way to produce the plateau effects.
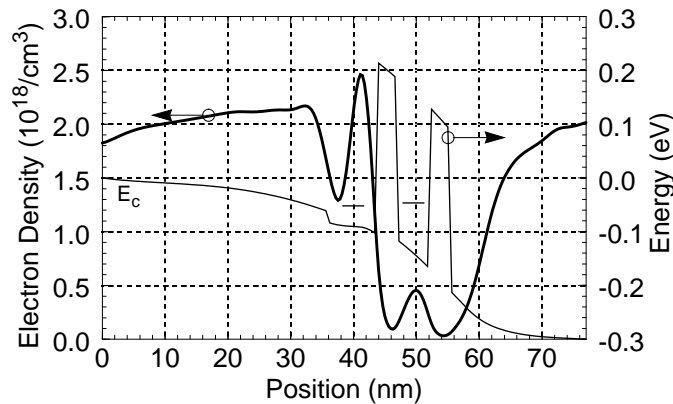
Figure 15: Conduction band and carrier density profiles for modified JB RTD operating in plateau (0.3 V). The emitter is modified with an 8 nm, 5% indium quantum well to deepen the emitter potential depression. Self-consistency is still the main cause of the emitter quantum well and thus plateau operation.
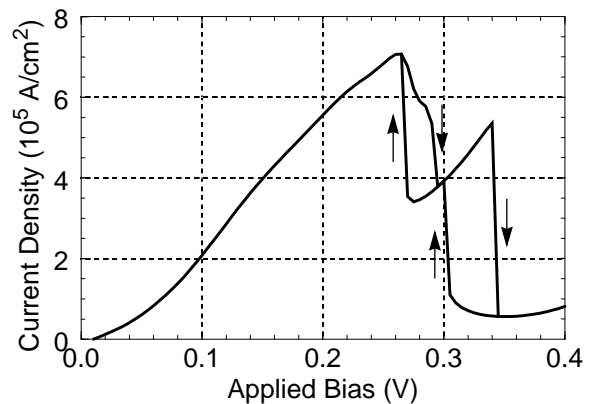
Figure 16: Simulated I-V curve of modified JB RTD of Figure 15 (compare to Figure 2). Note that the plateau effects are strong, even though the emitter layer is wide, in contrast to Figure 11. Also, a second hysteresis loop is has opened under the main current peak.
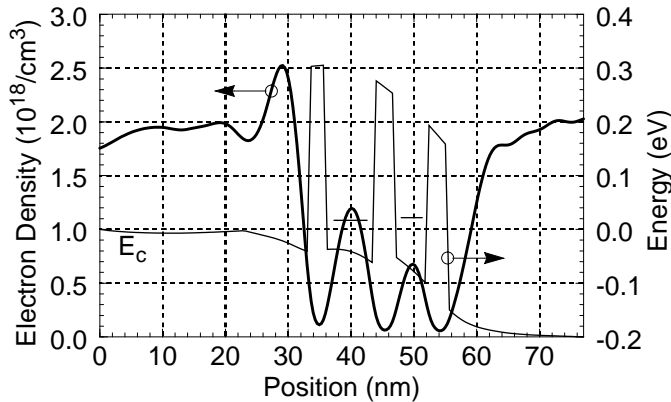
Figure 17: Conduction band and carrier density profiles for triple-barrier JB RTD operating in plateau. A third tunnel barrier has been placed in the emitter, creating an 8 nm quantum well. The lowest energy level of the new quantum well supplys electrons in a narrow energy band into the original quantum well.
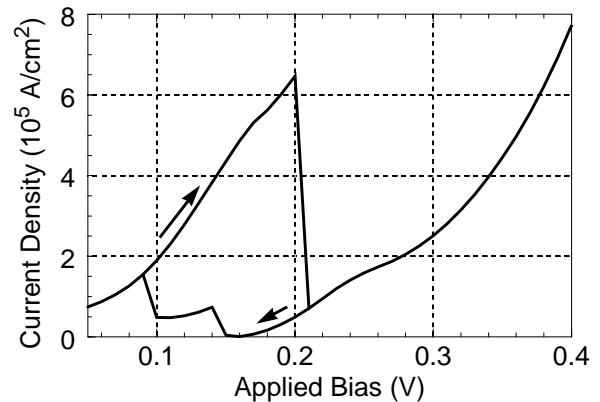
Figure 18: The high correlation of charge density in the two quantum wells of the triple-barrier JB RTD causes a very strong hysteresis and bistability. Unlike the original JB RTD, this hysteresis loop is under the main current peak, as in most measurements of this phenomenon. The plateau has disappeared.

5. SUMMARY

This work presented a detailed and comprehensive numerical simulation investigation of the physics behind some very intriguing transient Wigner function simulations of an RTD, published in 1991 by Jensen and Buot (JB). The simulations in this work produced several new insights into the physics of an I-V plateau in the NDR region of operation and associated intrinsic hysteresis, bistability, and high-frequency oscillations in this RTD. For example, steady-state simulations showed that the I-V plateau, previously ascribed to dynamic effects, is actually an equilibrium phenomenon. The physics of this I-V plateau were described in detail. During plateau operation, two parallel current paths are active. Electrons in the first current path scatter into a discrete quantum state in a potential depression in the emitter, and from there are transmitted through the quantum well state. The second current path is composed of electrons which tunnel directly through the lowered double barrier structure without scattering. Both of these current components are significant in creating the I-V plateau, along with its hysteresis and intrinsic bistability. The previously misdiagnosed cause of the positive slope of the plateau was also corrected.

The transient Wigner function simulations of the JB RTD presented also produced new insights. The I-V plateau was shown to be only partly unstable, while previous results concluded that the entire plateau was unstable. In fact, because the plateau was shown to be an equilibrium feature, only the NDR portion of the plateau could be unstable. Previous descriptions of the cause of the plateau oscillations were largely confirmed: self-consistent interaction of the charge in the emitter and quantum well, resulting in out-of-phase oscillations of these charges. One new discovery was that a discrete energy state in the emitter is required to produce the oscillations and the abrupt termination of the plateau. It was the oscillation in alignment of the discrete states in the emitter and quantum well that modulated the current.

Finally, the plateau effects were shown to be very sensitive to temperature and the assumed electron scattering rate. Therefore, simulations of modified resonant tunneling structures attempted to produce these potentially useful effects more robustly. Various approaches were considered or simulated in an attempt to produce the necessary double-moded electron distribution in the emitter, but these attempts were largely unsuccessful in improving on the simple JB RTD. In spite of this, with the virtually unlimited array of structural variations available, it is quite possible that a device which improves on the JB RTD can be found. In any event, based on the potential usefulness of the plateau effects simulated in the JB RTD, more accurate simulations require improvements in the scattering and contact models, both of which play key roles in the occurrence of these effects.

6. ACKNOWLEDGEMENTS

7. REFERENCES

[1] L. L. Chang and R. Tsu. "Resonant tunneling in semiconductor double barriers." *Applied Physics Letters*, 24(12):593–595, 1974.

[2] F. Capasso, K. Mohammed, and A. Y. Cho. "Resonant tunneling through double barriers, perpendicular quantum transport phenomena in superlattices, and their device applications." *Journal of Quantum Electronics*, 22(9):1853–1868, 1986.

[3] S. Luryi. "Observation of intrinsic bistability in resonant tunneling diode modeling." In F. Capasso and G. Margaritondo, editors, *Heterojunction Band Discontinuities: Physics and Device Applications*, chapter 12. Elsevier Science Publishers, 1987.

[4] F. Capasso, S. Sen, F. Beltram, L. M. Lunardi, A. S. Vengurlekar, P. R. Smith, N. J. Shah, R. K. Malik, and A. Y. Cho. "Quantum functional devices: Resonant-tunneling transistors, circuits with reduced complexity, and multiple-valued logic." *IEEE Transactions on Electron Devices*, 36(10):2065–2082, 1989.

[5] T. C. L. G. Sollner. "Comment on 'observations of intrinsic bistability in resonant-tunneling structures'." *Physical Review Letters*, 59(14):1622, 1987.

[6] J. F. Young, B. M. Wood, H. C. Liu, M. Buchanan, and D. Landheer. "Effect of circuit oscillations on the dc current-voltage characteristics of double barrier resonant tunneling structures." *Applied Physics Letters*, 52(17):1398–1400, 1988.

[7] H. C. Liu. "Simulation of extrinsic bistability of resonant tunneling structures." *Applied Physics Letters*, 53(6):485–486, 1988.

[8] E. R. Brown, J. R. Sˆderstrˆm, C. D. Parker, L. J. Mahoney, K. M. Molvar, and T. C. McGill. "Oscillations up to 712 GHz in InAs/AlSb resonant-tunneling diodes." *Applied Physics Letters*, 58(20):2291–2293, 1991.

[9] M. A. Reed, J. W. Lee, R. K. Aldert, and A. E. Wetsel. "Investigation of quantum well and tunnel barrier growth by resonant tunneling." *Journal of Materials Research*, 1(2):337–342, 1986.

[10] E. S. Alves, L. Eaves, M. Henini, O. H. Hughes, M. L. Leadbeater, F. W. Sheard, G. A. Toombs, G. Hill, and M. A. Pate. "Observation of intrinsic bistability in ressonant tunneling devices." *Electronics Letters*, 24(18):1190–1191, 1988.

[11] A. Zaslavsky, V. J. Goldman, and D. C. Tsui. "Resonant tunneling and intrinsic bistability in asymmetric double-barrier heterostructures." *Applied Physics Letters*, 53(15):1408–1410, 1988.

[12] M. L. Leadbeater, E. S. Alves, L. Eaves, M. Henini, O. H. Hughes, F. W. Sheard, and G. A. Toombs. "Charge build-up and intrinsic bistability in an asymmetric resonant-tunnelling structure." *Semiconductor Science and Technology*, 3:1060–1062, 1988.

[13] K. L. Jensen and F. A. Buot. "Numerical simulation of intrinsic bistability and high-frequency current oscillations in resonant tunneling structures." *Physical Review Letters*, 66(8):1078–1081, 1991.

[14] F. A. Buot and K. L. Jensen. "Intrinsic high-frequency oscillations and equivalent circuit model in the negative differential resistance region of resonant tunneling devices." *COMPEL*, 10(4):241–253, 1991.

[15] F. A. Buot. "Mesoscopic physics and nanoelectronics: Nanoscience and nanotechnology." *Physics Reports*, 234(2-3):73–174, 1993.

[16] F. A. Buot and A. K. Rajagopal. "High-frequency behavior of quantum-based devices: Equivalent-circuit, nonperturbative-response, and phase-space analyses." *Physical Review B*, 48(23):17217–17232, 1993.

[17] F. A. Buot and A. K. Rajagopal. "Theory of novel nonlinear quantum transport effects in resonant tunneling structures." *Materials Science and Engineering*, B35(1-3):303–317, 1995.

[18] D. L. Woolard, F. A. Buot, D. L. Rhodes, X. Lu, and B. S. Perlman. "An assessment of potential nonlinear circuit models for the characterization of resonant tunneling diodes." *IEEE Transactions on Electron Devices*, 43(2):332–341, 1996.

[19] D. L. Woolard, F. A. Buot, D. L. Rhodes, X. J. Lu, R. A. Lux, and B. S. Perlman. "On the different physical roles of hysteresis and intrinsic oscillations in resonant tunneling structures." *Journal of Applied Physics*, 79(3):1515–1525, 1996.

[20] W. R. Frensley. "Wigner-function model of a resonant-tunneling semiconductor device." *Physical Review B*, 36(3):1570–1580, 1987.

[21] F. A. Buot and K. L. Jensen. "Lattice Weyl-Wigner formulation of exact many-body quantum-transport theory and applications to novel solid-state quantum-based devices." *Physical Review B*, 42(15):9429–9457, 1990.

[22] R. Tsu and L. Esaki. "Tunneling in a finite superlattice." *Applied Physics Letters*, 22(11):562–564, 1973.

[23] C. M. Tan, J. Xu, and S. Zukotynski. "Study of resonant tunneling structures: A hybrid incremental Airy function plane-wave approach." *Journal of Applied Physics*, 67(6):3011–3017, 1990.

[24] B. A. Biegel and J. D. Plummer. "Comparison of self-consistency iteration options for the Wigner function method of quantum device simulation." *Physical Review B*, 54(11):8070–8082, 1996.

[25] B. A. Biegel and J. D. Plummer. "Applied bias slewing in transient wigner function simulation of resonant tunneling diodes." *IEEE Transactions on Electron Devices*, 44(5):733–737, 1997.

[26] K. L. Jensen and F. A. Buot. "The effects of scattering on current-voltage characteristics, transient response, and particle trajectories in the numerical simulation of resonant tunneling diodes." *Journal of Applied Physics*, 67(12):7602–7607, 1990.

[27] B. A. Biegel. *Quantum Electronic Device Simulation*. PhD thesis, Stanford University, Mar. 1997.

[28] B. Ricco and M. Y. Azbel. "Physics of resonant tunneling. the one-dimensional double-barrier case." *Physical Review B*, 29(4):1970–1981, 1984.

[29] C. Y. Belhadji, K. P. Martin, J. J. L. Rascol, R. J. Higgins, R. C. Potter, H. Hier, and E. Hempfling. "Bias circuit effects on the current-voltage characteristic of double-barrier tunneling structures: Experimental and theoretical results." *Applied Physics Letters*, 57(1):58–60, 1990.

[30] C. R. Wallis and S. W. Teitsworth. "Conditions for current oscillations and hysteresis in resonant tunneling diode circuits." In *Proceedings of the International Semiconductor Device Research Symposium*, pages 487–490, University of Virginia, Charlottesville, 1993. Engineering Academic Outreach.

[31] C. R. Wallis and S. W. Teitsworth. "Hopf bifurcations and hysteresis in resonsant tunneling diode circuits." *Journal of Applied Physics*, 76(7):4443–4445, 1994.

[32] Private conversation with K. L. Jensen.

[33] W. R. Frensley. "Effect of inelastic processes on the self-consistent potential in the resonant-tunneling diode." *Solid State Electronics*, 32(12):1235–1239, 1989.

[34] K. L. Jensen and F. A. Buot. "The methodology of simulating particle trajectories through tunneling structures using a Wigner distribution approach." *IEEE Transactions on Electron Devices*, 38(10):2337–2347, 1991.

[35] V. J. Goldman, D. C. Tsui, and J. E. Cunningham. "Observation of intrinsic bistability in resonant-tunneling structures." *Physical Review Letters*, 58(12):1256–1259, 1987.

[36] N. Tabatabaie and M. C. Tamargo. "Determination of elastic tunneling traversal times." In *International Elestron Devices Meeting (IEDM) Technical Digest*, pages 80–83, 1986.

[37] C. R. Wie and Y. W. Choi. "Designing resonsant tunneling diode structures for increased peak current density." *Applied Physics Letters*, 58(10):1077–1079, 1991.

[38] J. S. Wu, C. Y. Chang, C. P. Lee, K. H. Chang, D. G. Liu, and D. C. Liou. "Resonant tunneling of electrons from quantized levels in the accumulation layer of double-barrier heterostructures." *Applied Physics Letters*, 57(22):2311–2312, 1990.